Journal of Cancer Research and Clinical Oncology (2019) 145:1123–1132
https://doi.org/10.1007/s00432-019-02857-8

ORIGINAL ARTICLE – CANCER RESEARCH

CIK cell-based delivery of recombinant adenovirus KGHV500 carrying the anti-p21Ras scFv gene enhances the anti-tumor effect and safety in lung cancer

Xin-Rui Lin[1,2] · Xin-Liang Zhou[3] · Qiang Feng[2] · Xin-Yan Pan[2] · Shu-Ling Song[2] · Hong Fang[2] · Jin Lei[2] · Ju-Lun Yang[1,2,3]

Received: 30 August 2018 / Accepted: 6 February 2019 / Published online: 22 February 2019
© Springer-Verlag GmbH Germany, part of Springer Nature 2019

Abstract

Purpose Adenovirus (Ads) is one of the most popular vectors used in gene therapy for the treatment of cancer. However, systemic therapy is limited by circulating antiviral antibodies and poor viral delivery in vivo. In this study, we used cytokine-induced killer (CIK) cells as delivery vehicles of Ads KGHV500 carrying the anti-p21Ras scFv gene to treat Ras gene-related lung cancer and investigate the anti-tumor effect in vitro and in vivo.

Methods The human lung cancer cell line A549 was employed to investigate the anti-tumor activity of recombinant Ads KGHV500 harboring the anti-p21Ras scFv gene using MTT, wound healing, transwell invasion, and apoptosis assays in vitro. Next, CIK cells were used as delivery vehicles to deliver KGHV500 carrying the anti-p21Ras scFv gene to treat A549-transplanted tumors in nude mice, and viral replication, p21Ras scFv expression, and the therapeutic efficacy were assessed.

Results In vitro studies showed that KGHV500 had potent anti-tumor activity. In addition, in vivo, this combination therapy significantly inhibited the growth of lung cancer xenografts compared with mice treated with KGHV500 alone. KGHV500 and anti-p21Ras scFv were observed in tumor tissue, but were nearly undetectable in normal tissues.

Conclusions The co-delivery of anti-p21Ras scFv by CIK cells and KGHV500 could increase the anti-tumor effect and safety, and possess considerable advantages for the treatment of Ras-related cancer.

Keywords CIK cells · Carrier · Adenovirus · Anti-p21Ras scFv · Lung cancer · Therapy

Introduction

Lung cancer, accounting for approximately 26% of all cancer deaths, represents the major cause of cancer-related mortality worldwide (Siegel et al. 2017; Ferlay et al. 2015). The traditional treatment for lung cancer is aggressive surgical debulking followed by chemotherapy or radiation. Most lung cancers are diagnosed at a late advanced stage in patients, are not suitable for surgery, and are difficult to cure (Crino et al. 2010). In the last decades, some targeted drugs have been approved for the clinical treatment of lung cancer (Lara-Guerra and Roth 2016), such as crizotinib that targets anaplastic lymphoma kinase (ALK) (Casaluce et al. 2016) and gefitinib that targets epidermal growth factor receptor (EGFR) (Osborne et al. 2011). However, the response rate of crizotinib was reported to be 65% (Shaw et al. 2013) and that of gefitinib was less than 25% (Kohler and Schuler 2013), and some patients easily develop resistance. Thus, developing targeting drugs for the other molecular alterations, including Ras gene mutation, is imminent.

The Ras gene encoding the p21 Ras protein is the earliest human proto oncogene (Parada et al. 1982; Lowy and Willumsen 1993). Numerous studies have shown that Ras mutation is an early event in the development of cancer,

Xin-Rui Lin and Xin-Liang Zhou have contributed equally to this work.

✉ Ju-Lun Yang
yangjulun@sina.com

[1] Graduate School, Kunming Medical University, Chenggong District, Kunming, People's Republic of China

[2] Department of Pathology, 920th Hospital of the Joint Logistics Support Force of PLA, 212 Daguan Road, Kunming 650032, Yunnan, People's Republic of China

[3] Department of Pathology, Medical Faculty, Kunming University of Science and Technology, Kunming, People's Republic of China

including lung cancer (Johnson et al. 2001; Kim et al. 2005). Previously, we prepared a single-chain fragment variable antibody (scFv) to p21Ras that could react specifically with wild-type and mutant p21Ras proteins in tumor cell lines and primary tumors (Yang et al. 2016). Further studies demonstrated that recombinant Ads carrying the anti-p21Ras scFv gene, KGHV300, could enter tumor cells, and replicate and intracellularly express anti-p21Ras scFv. Intratumoral injection of KGHV300 could inhibit the growth of nude mouse xenografts (Pan et al. 2017). However, KGHV300 could not be transported to tumors by intravenous injection, because it could infect normal cells. Thus, we constructed recombinant Ads KGHV500 that not only carries the anti-p21Ras scFv gene but also can bind to cytokine-induced killer (CIK) cells (unpublished data). In this study, we used CIK cells as delivery vehicles of KGHV500 to treat Ras gene-related lung cancer and investigate the anti-tumor effect in vitro and in vivo.

Materials and methods

Cell lines and cell culture

The human lung cancer cell line A549 was obtained from American Type Culture Collection (ATCC), and it contains a mutation at exon 2 in codon 12 of the K-ras gene (Okudela et al. 2004). The human embryonic kidney (HEK) 293 cell line was purchased from Microbix Biosystem (Toronto, ON, Canada). These cells were cultured, according to the ATCC guidelines, in RPMI 1640 medium (HyClone, Inc, USA) containing 10% heat-inactivated fetal bovine serum (FBS) (Biological Industries, Israel), 100 U ml^{-1} of penicillin, and 100 μg/ml of streptomycin under a 5% CO_2 atmosphere at 37 °C. Recombinant Ads (Ads) receptor CD46, which can bind the Ad35 fiber of KGHV500 and KGHV400, was detected on the membrane of A549 cells by immunohistochemistry (IHC).

Recombinant adenovirus

Recombinant Ads KGHV500 and KGHV400 were constructed by our laboratory and contained the green fluorescent protein (GFP) gene. In both, the cilia gene was replaced with the Ad35 cilia gene, so that they can bind the CD46 molecule on the surface of CIK cells and tumor cells. KGHV500 contains the anti-p21Ras scFv gene but not KGHV400. KGHV500 and KGHV400 were propagated in HEK293 cells, purified twice by CsCl gradient centrifugation (Ostapchuk et al. 2011), and stored at − 80 °C. Viral titers were determined using the Tissue Culture Infectious Dose50 (TCID50) method (Yu et al. 2011).

Recombinant adenovirus-infected tumor cells

To test the infection efficiency, 1×10^6 A549 cells per well (6-well plate) were seeded at 37 °C with 5% CO_2. When 80% of confluent cells were formed, KGHV500 was added into the wells at MOIs of 50, 100, and 200. After 48 h, GFP-positive cells were detected under a fluorescence microscope (Nikon, Tokyo, Japan). At the same time, the co-cultured cells were fixed in 2.5% glutaraldehyde and cut into ultrathin slices (Munn et al. 1985), and then, the Ads in tumor cells were observed by electron microscopy (EM) (JEM-1011, Japan).

Preparation and identification of CIK cells

Human peripheral blood mononuclear cells (PBMCs) were isolated from healthy volunteers as described previously (Finke et al. 1998). PBMCs were incubated in RPMI 1640 medium-containing 10% FBS. To obtain CIK cells, the nonadherent cells were collected and activated with 1,000 U/mL of IFN-γ (PeproTech, NJ, USA) in RPMI 1640 at 37 °C for 24 h, followed by the addition of 50 ng/ml of CD3 monoclonal antibody and 300 U/ml of IL-2 (PeproTech, NJ, USA). The cells were kept at 1×10^6 cells/ml in 37 °C with 5% CO_2 and were subcultured every 3 days in fresh complete medium and 300 U/ml of IL-2. The CIK cells were obtained at day 14. IHC was used to detect the expression of CD3, CD46, and CD56 on the surface of the cells to identify CIK cells.

Combination between CIK cells and recombinant adenovirus

At day 14, CIK cells were infected with KGHV500 at an MOI of 100 for 48 h, and the Ads hexon protein was detected by IHC to identity the binding of CIK cells to KGHV500.

Cell killing assay

Adenovirus-induced cell death was assessed using the MTT assay. Logarithmic growth phase cells were inoculated at a density of 1×10^4 cells per well in 96-well plates and were maintained under appropriate conditions. After 24 h, the cells were infected with recombinant Ads at an MOI of 100, and the control group was treated with an equal amount of RPMI1640 culture medium. At 1, 2, 3, 4, and 5 days after infection, 20 μl of MTT (5 mg/ml) was added into each well. After 4 h of incubation with MTT, DMSO (100 μl/well) was added, and the plates were shaken for 10 min. The optical

density (OD) value of each well was measured at 490 nm using a microplate reader (Bio-Rad, Model 680).

Wound healing assay

A549 cells were cultured in 6-well plates until 80% fusion and then were starved in serum-free medium overnight. Thereafter, the bottom of the culture plates was scratched with a 200-μl tip head, followed by washing three times with PBS. KGHV500 or KGHV400 was added to cells at an MOI of 100; 5% serum medium represented the negative control group. Cell migration was detected under an inverted microscope (Olympus, Japan) at 0 h, 24 h, and 48 h, and the migration area was calculated using the ImageJ software.

Transwell invasion assay

A549 cells were plated into 24-well plates. Next, the cells were cultured until the 80% fusion state and then were starved in serum-free medium for 12 h. Thereafter, recombinant Ads KGHV500, KGHV400, and PBS were added to the cells at an MOI of 100, followed by continuous culture for 24 h. Next, 200 μl of the cell suspension (1×10^5) was added to a Transwell chamber (8-μm pore size; Corning, NY, USA), which contained 100 μl of Matrigel (BD, USA); 600 μl of RPMI-1640 supplemented with 10% FBS was added to the lower chamber as a chemoattractant. After 24-h incubation with 5% CO_2 at 37 °C, the cells in the upper surface of the insert membrane were removed by wiping with a cotton swab, and the cells in the lower surface were counted under a microscope after methanol fixation and Giemsa staining.

Animal model and in vivo experiments

The subcutaneous xenograft model was established by the inoculation of 10^7 A549 cells into the right flank of 4-week-old female BALB/c nude mice (Vital River Laboratories, Beijing, China). CIK cells carrying KGHV500 were prepared by co-culturing CIK cells with KGHV500 at an MOI of 100 for 48 h.

When the tumors had grown to an average diameter of 0.5 cm, the animals were assigned randomly to five groups, 25 nude mice per group. For the CIK + KGHV500 group, 1×10^7 CIK cells combined with 2×10^8 IFUs of KGHV500 were injected into the tail vein. For the CIK + KGHV400 group, 1×10^7 CIK cells combined with 2×10^8 IFUs of KGHV400 were injected into the tail vein. In the KGHV500, KGHV400, or PBS group, KGHV500, KGHV400, or PBS was injected into the tail vein by intravenous injection, respectively. Tumor growth was measured using a Vernier caliper every 3 days. The tumor volume (mm^3) was calculated using the following formula: (length × width^2)/2. Tumor growth curves were drawn using these data.

Two tested mice of each group were randomly selected and killed to harvest tumors and tissues at 1, 2, 3, 5, and 7 days. To determine the safety of this treatment, the distribution of KGHV500 in normal tissues was observed by IHC. Next, western blotting was used to detect the change in KGHV500 in the tumor for a week; at the same time, scFv was detected to observe the expression of exogenous effector proteins.

On day 34, the xenografts of the PBS group were ulcerated, the mice were sacrificed, and the tumors and normal tissues were excised to prepare paraffin blocks or freeze for biology examination. To further verify the effectiveness of the treatment, we examined anti-p21Ras scFv in relevant tissues by western blotting (WB) on the 34th day.

Western blot assay

WB was performed as described previously (Yang et al. 2016a, b) by extracting protein from tissue samples, followed by electrophoresis on SDS-PAGE gels and transfer of proteins to polyvinylidene fluoride (PVDF) membranes. Next, the PVDF membranes were incubated with primary antibody (ZSGB-Bio, TA-09, China) after blocking and then were incubated with goat anti-mouse IgG and horseradish peroxidase (HRP) (ZSGB-Bio, ZB-5305, China). The PVDF membranes were then stained with DAB. β-Actin protein was used as an internal control. Images were converted to the grayscale mode in Photoshop software. Quantification of the target proteins was accomplished by calculating the relative band intensity in the grayscale images of the proteins (scFv/β-Actin or Hexon/β-Actin) (Yan et al. 2015).

Apoptosis assay

Tissues at day 34 after injection and cells co-cultured with recombinant Ads for 48 h were cut into sections, and apoptotic cells were detected using the terminal deoxynucleotidyl transferase dUTP nick end labeling (TUNEL) assay (In Situ Cell Death Detection Kit; Roche Diagnostics); normal cell nuclei were stained with 4′, 6-diamidino-2-phenylindole (DAPI). Staining was conducted according to the manufacturer's recommendations.

Quantitative real-time PCR (qRT-PCR) was used to determine the expression of the apoptosis-related genes caspase-3, caspase-7, Bcl-2, p53, and survivin. After treatment for 34 days, total RNA was purified from tumor tissues using the Eastep™ Total RNA Extraction kit (Promega, Madison, WI, USA). Total RNA (5 μg) was used for reverse transcription using the GoScript™ Reverse Transcription system (Promega, Madison, WI, USA). Apoptosis-related genes used the corresponding primers, and the internal

standard was glyceraldehyde-3-phosphate dehydrogenase (GAPDH), which used the primers GAPDH-F/GAPDH-R. Every reaction series included a negative control with no template. The PCR amplification products were separated by 1% agarose gel electrophoresis and were observed by SYBR Green staining (Bio-Rad). The data were analyzed using Bio-Rad CFX96 Manager software.

Data analysis

All in vitro experiments were performed in triplicate. Each value is expressed as the means ± standard deviation (SD), and the statistical analysis of the results in MTT assay, wound healing assay, growth curve, and grayscale value of WB was performed using one-way analysis of the variance (ANOVA) followed by replicate measures. The statistical analysis of the results in transwell invasion assay, apoptosis assay, and qRT-PCR was performed using one-way analysis (ANOVA) followed by least significant difference (LSD-T). All the data were analyzed using the SPSS 24.0 software package, and statistical significance was indicated by a P value < 0.05.

Results

Infectious capability of recombinant adenovirus to A549 cells and CIK cells

The IHC assay showed that the expression of CD46 in A549 cells approached 100% (Fig. 1a). Cells with GFP were observed at an MOI of 100, far more than at the MOIs of 50 and 200 (Fig. 1b); an MOI of 100 had the best infection efficiency. In addition, A549 cells were observed by EM, and Fig. 1c shows that numerous Ads particles were present in both the nucleus and cytoplasm of A549 cells, confirming that KGHV500 can infect A549 effectively and replicate in cells.

After 14 days of culture with IL-2, IFN-γ, and CD3 monoclonal antibody, the CIK cells were induced and the cell number was more than that on day 1. IHC showed the expression of CD3- and CD56-positive cells approaching 95% or 15% (Fig. 1d), respectively, and these data were consistent with those in a previous report (Yang et al. 2012), demonstrating that CIK cells were successfully

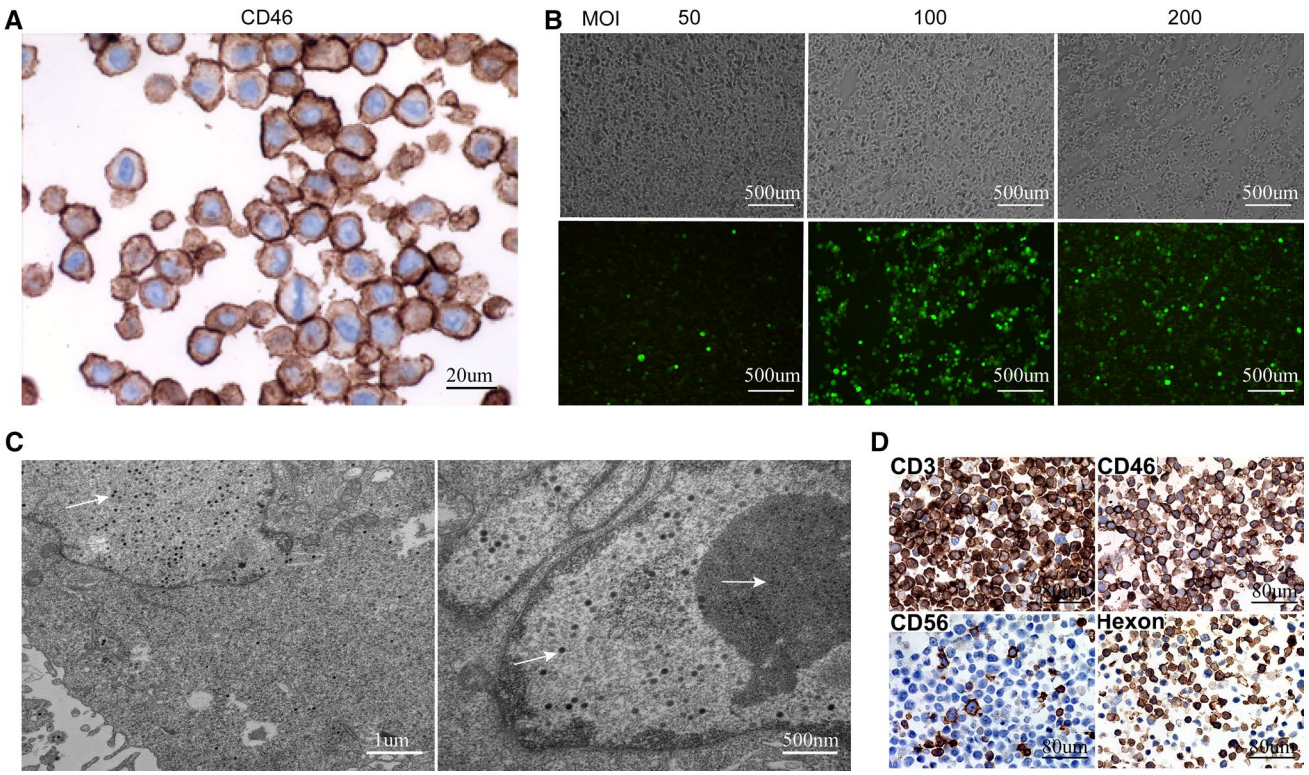

Fig. 1 KGHV500-infected A549 cells and CIK cells. **a** CD46 is a receptor of recombinant adenovirus that mediates the combination of KGHV500 and target cells. IHC analysis showed that CD46 is highly expressed on the surface of A549 cells (×400). **b** A549 cells were treated with KGHV500 at different MOIs for 48 h. The green fluorescence signals were detected by microscopy (×100); an MOI of 100 was the best infection efficiency. **c** Many virus particles were scattered throughout the cytoplasm and nucleus. **d** IHC analysis showed that CIK cell markers (CD3, CD46, and CD56) were expressed on the surface of CIK cells, and hexon expression in KGHV500 was detected in CIK cells (×200)

induced. In addition, the percentage of CD46 on the CIK cell membrane surface was approximately 100% by the cell number count (Fig. 1d). After the co-culture of CIK cells and KGHV500, 78% of CIK cells were Ads hexon positive (Fig. 1d); thus, KGHV500 could effectively bind to CIK cells.

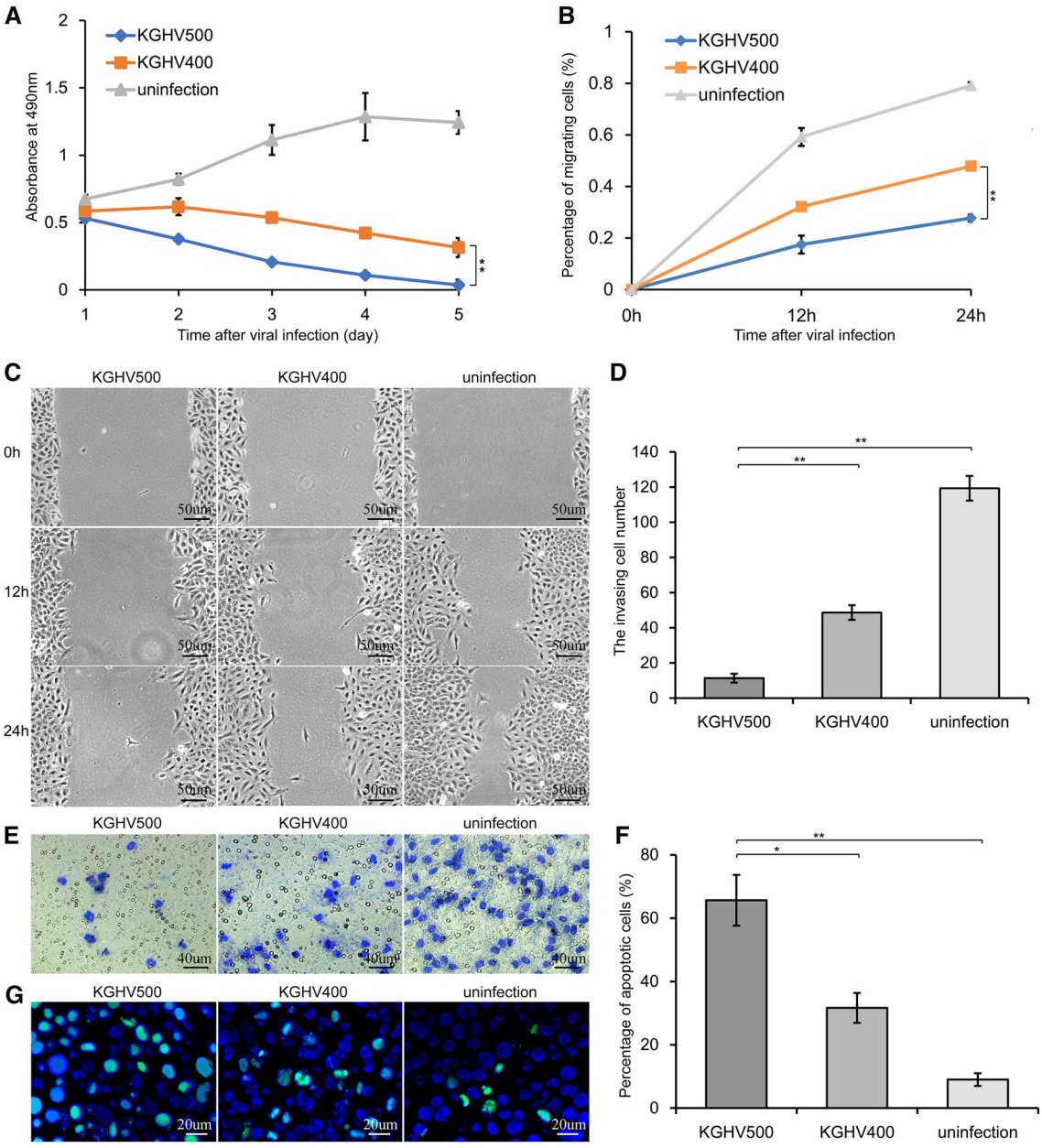

Fig. 2 Anti-tumor biological activities of KGHV500 in vitro. **a** MTT assay to measure cell killing in A549 cells treated with KGHV500 and KGHV400. The absorbance values in the KGHV500 group were lower than that in the control group. **b, c** Cell migration was observed at 12 h and 24 h after scratching and infection by KGHV500 and KGHV400 (×100). The migration areas of the KGHV500 group were smaller than those of the KGHV400 and PBS groups. **d, e** Transwell assays observed the inhibition of invasiveness. Fixed and stained cells of the membrane were counted. The number of invading A549 cells in the KGHV500 group was much lower than that of the other two groups. **f, g** Apoptotic tumor cells of different groups were detected by TUNEL staining (green fluorescence), and nuclei were detected by DAPI staining (blue fluorescence) (×1000). The number of apoptotic cells in the KGHV500 group was markedly greater than that in the control group. All experiments were performed in triplicate. All the data are represented as the means ± standard deviation (SD) of three experiments. *$P < 0.05$; **$P < 0.01$

Anti-tumor effect of KGHV500 in vitro

MTT assays were performed to evaluate the potential killing effects of KGHV500 in A549 cells. According to the curve position in Fig. 2a, the average number of live cells in the uninfected group continued to increase. However, in the KGHV500-infected group, the average number of live cells steadily declined after 24 h, even more sharply than that in the KGHV400-infected group. There was a significant difference among the data of the three groups ($P < 0.01$), indicating that KGHV500 could significantly inhibit the growth and proliferation of A549 tumor cells.

We compared the migration, invasion, and apoptosis abilities of A549 cells between the KGHV500- and KGHV400-infected groups. Figure 2b, c shows that the area of migrating cells in the uninfected and KGHV400-infected groups was larger than that in the KGHV500 group at 24 h and 48 h. As evidenced by the transwell invasion assay (Fig. 2d, e), KGHV500 infection could significantly inhibit the invasive ability of A549 cells compared with the KGHV400-infected and uninfected groups. In addition, the percentage of apoptotic A549 cells in the KGHV500-infected group was higher than that in the other group (Fig. 2f, g). These results showed clearly that infection by KGHV500 resulted in a stronger capacity to inhibit the migration, invasion, and apoptosis promotion of A549 cells.

Anti-tumor activity of KGHV500 combined with CIK cells in vivo

We treated human lung cancer A549 cell line xenografts by intravenous injection in the tail with CIK cells carrying KGHV500, CIK cells carrying KGHV400, KGHV500, CIK cells, or PBS. The xenograft tumor growth curves are shown in Fig. 3a. In the PBS-treated control group, xenografts grew rapidly. In the KGHV500-treated group, CIK-treated group, CIK + KGHV400-treated group, and CIK + KGHV500-treated group, the growth rate of the tumors decreased ($P < 0.01$). The growth of the xenografts in the CIK + KGHV500-treated group was slowest. These results indicated that KGHV500 combined with CIK cells

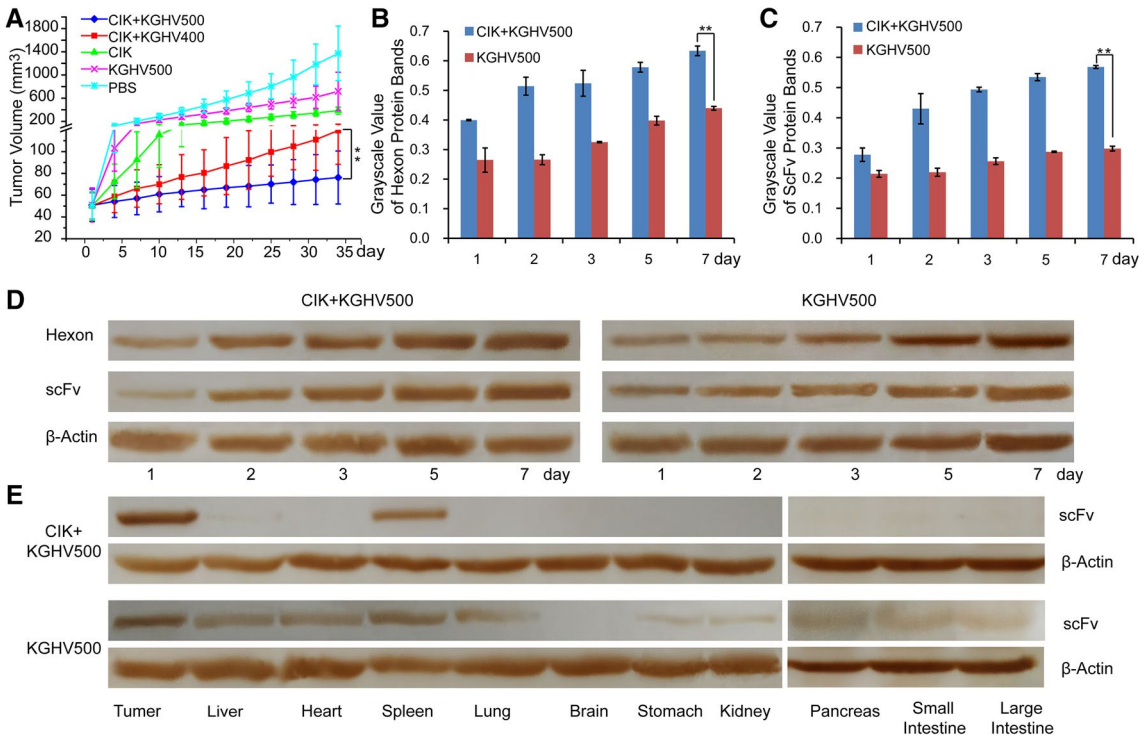

Fig. 3 Anti-tumor activity against human lung cancer A549 cell line xenografts in nude mice. **a** After treatment, the tumor volume was measured every 3 days, and the therapeutic effects were compared by drawing growth curves. The tumor volumes of the CIK + KGHV500 group were much smaller than those of the other groups. The data points are expressed as the means ± SD of the tumor volumes. **b, c** The changing trends of the grayscale value in **d** were evaluated and depicted. **d** KGHV500 and anti-p21Ras scFv expression in the tumors of the CIK + KGHV500 and KGHV500 groups was detected by WB for 7 days. Hexon protein expression in CIK + KGHV500 increased with time, and the increasing trend was higher than that in the KGHV500 group. In addition, scFv was continuously expressed in tumors and increased gradually, and CIK + KGHB500 had a higher scFv content. **e** Detection of scFv expression in various tissues at day 34. scFv expression could only be detected in tumor and spleen tissues in the CIK + KGHV500 group and in all tissues except the brain in the KGHV500 group. *$P < 0.05$; **$P < 0.01$

can obviously inhibit the growth of the xenograft tumors compared with the other groups.

Expression of hexon and scFv in vivo

To examine hexon expression in KGHV500 and anti-p21Ras scFv expression in the tumor tissues of the CIK + KGHV500 and KGHV500 groups, we observed the protein expression in tumor tissues by WB for a week (Fig. 3d). As shown in Fig. 3b, the grayscale value of the hexon protein in the CIK + KGHV500 group increased over time and that in the CIK + KGHV500 group was more than that in the KGHV500 group at all times ($P < 0.01$). Thus, CIK cells can carry the KGHV500 to tumor cells. The grayscale value of scFv in Fig. 3c showed that scFv was continuously expressed in tumors and was increased gradually in the CIK + KGHV500 group, and the change trend of scFv was more notable than that in the KGHV500 group. To verify whether scFv was continuously expressed in tumors, we detected scFv in tumors at day 34 by WB and found that more scFv appeared in tumor tissue in the CIK + KGHV500 group than in the KGHV500 group, and almost no scFv was detected in normal tissues except in the spleen because of the spleen homing of lymphocytes.

KGHV500 in important organs

To test the safety of CIK cells carrying KGHV500, each relevant tissue in BALB/c mice was observed by IHC at day 7. Cells with positive hexon protein expression in the CIK + KGHV500 group were observed in the spleen and tumor tissues (Fig. 4). In addition, in the KGHV500-treated group, positive cells could be observed in every tissue which we checked except brain tissue, and hexon expression in each organ was not regular ($P > 0.05$). The result showed that CIK cells play important roles in raising the efficiency of targeting and improving the infection efficiency of KGHV500. Thus, the safety, effectiveness, and tumor-targeting of the combination treatments were as expected and without unexpected toxicities observed in normal tissue.

Apoptosis of tumor cells in vivo

After treatment for 34 days, the apoptosis rate of the tumor tissues was determined using the TUNEL

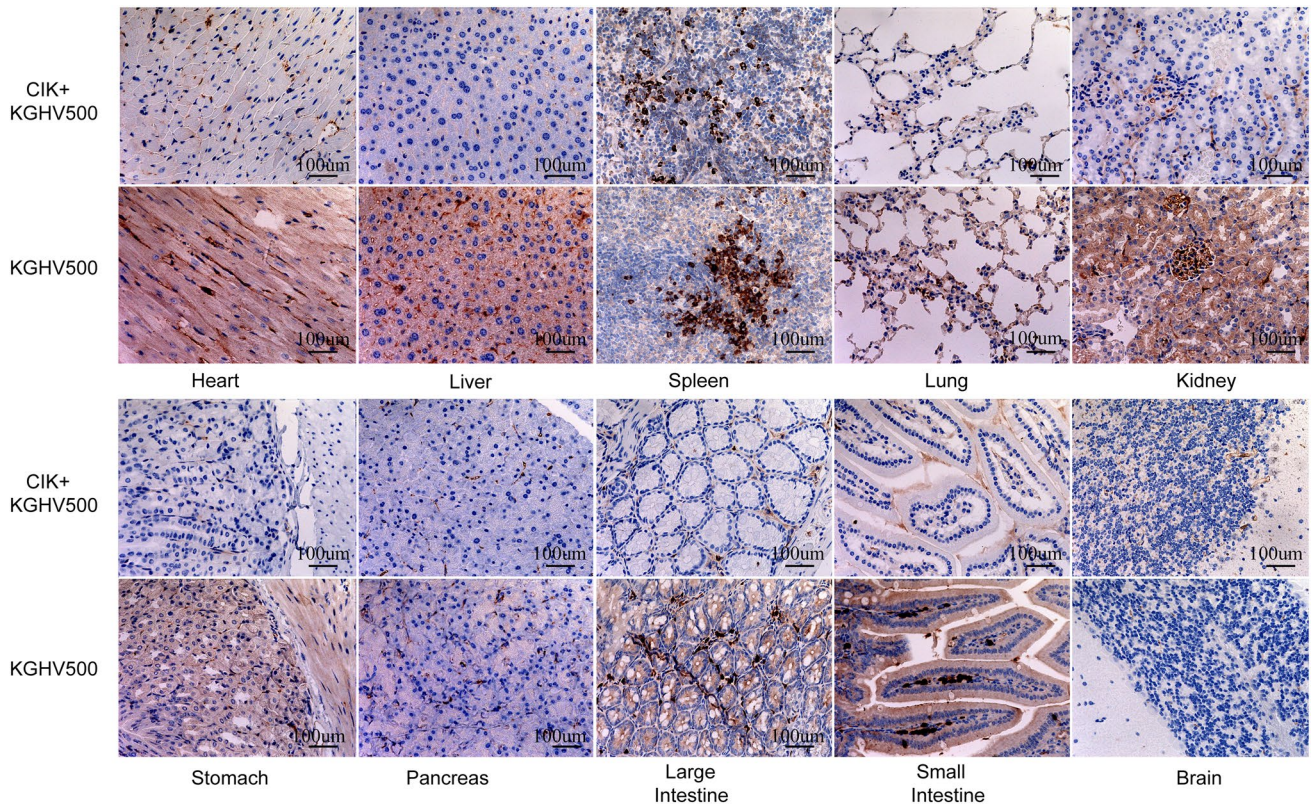

Fig. 4 Distribution of KGHV500 in vivo. Hexon expression in various tissues at day 7 was detected by IHC to track the virus. In the CIK + KGHV500 group, hexon expression was detected in tumor and spleen tissues. Because of the blood–brain barrier, hexon could not be detected in brain tissue of the KGHV500 group (×40). *$P < 0.05$; **$P < 0.01$

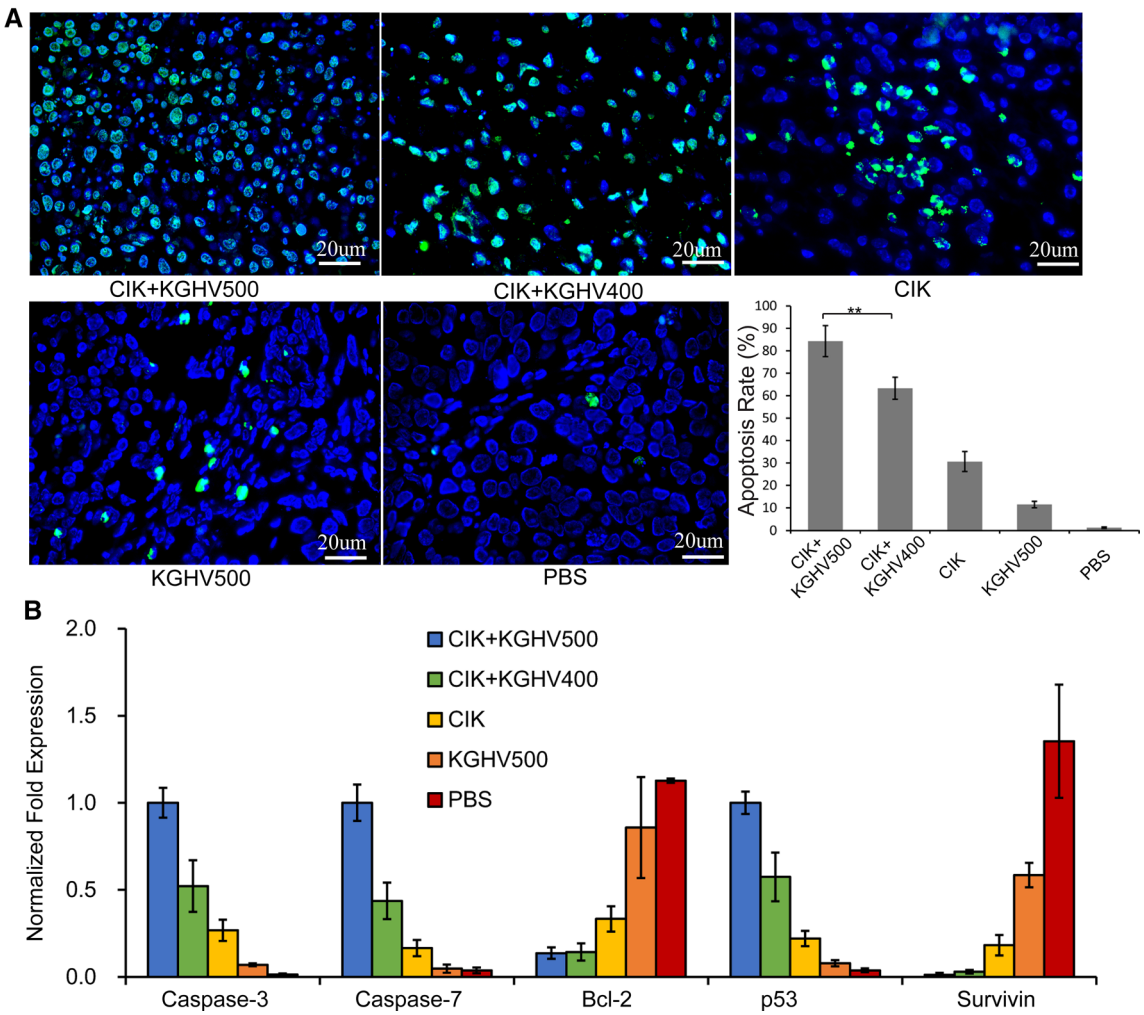

Fig. 5 Detection of the apoptosis-inducing capacity of CIK + KGHV500 in vivo. **a** The percentage of apoptotic cells in CIK + KGHV500 was more than that in the other groups. **b** The expression level of apoptotic genes was analyzed by the qRT-PCR. In the CIK + KGHV500 group, the expression of the proapoptotic genes caspase-3, caspase-7 and p53 was increased and that of the anti-apoptotic genes Bcl-2 and survivin was decreased. $^{*}P < 0.05$; $^{**}P < 0.01$

assay. More apoptotic tumor cells were observed in the CIK + KGHV500 group (96.9 ± 23.4) than in the CIK + KGHV400 group (80.3 ± 16.48) and other control groups (Fig. 5a).

Next, we performed qRT-PCR to measure the expression level of apoptosis-associated genes (Fig. 5b). Caspase-3, caspase-7, and p53 are proapoptotic genes that could induce cell apoptosis, while Bcl-2 and survivin are anti-apoptosis genes. The RNA expression of the proapoptotic genes was demonstrated to be the highest in the CIK + KGHV500 group, but less in the CIK + KGHV400, CIK and KGHV500 groups, and the least in the PBS group, while that of Bcl-2 and survivin showed an opposite tendency. The results of the apoptosis assay proved that the ability to induce apoptosis in the CIK + KGHV500 group is stronger than that in the other groups.

Therefore, KGHV500 combined with CIK cells can specifically recognize and enter the established tumor, and the expression of anti-p21Ras scFv can induce tumor cell apoptosis by binding to the p21Ras protein in tumor cells.

Discussion

Lung cancer is a complex disease caused by interactions among multiple genes, and the genetic alterations occur in oncogenes and tumor suppressor genes. Gene therapy for lung cancer against driver gene aberrations is one of the most revolutionary medical technologies that have been dramatically changed treatment strategies. Thus far, gene therapy drugs for lung cancer, including Ad-p53 (Gendicine) (Lara-Guerra and Roth 2016; Keedy et al. 2008) and

TUSC2 nanovesicles (Lu et al. 2012), have been in clinical trials for more than 10 years because their application has been limited by constraints on delivery, safety, and tumor-targeting. Identifying appropriate carriers is a critical issue for successful gene therapeutic approaches in patients. Commonly used gene therapy vectors include retroviruses (Urban and Merten 2011; Thomas et al. 2003), Ads (Kotterman et al. 2013; Qin et al. 2005), and chitosan (Köpinghöggård et al. 2001), among which Ads has shown the most clinical promise.

Ads is one of the most popular vectors of gene therapy and is extensively used in clinical experiments because of its high rate of transfection and expression (Kimura et al. 2013). However, systemic therapy using viral vectors is constrained by circulating antiviral antibodies and potential toxicity to normal tissue; thus, virus vectors are usually used in local therapy. For example, Ad-p53 was proven to be administered effectively and safely via bronchoalveolar lavage in patients with bronchioloalveolar lung carcinoma (Keedy et al. 2008), and Talimogene laherparepvec was used by intratumoral injection (Andtbacka et al. 2015).

Virus-infected cells can serve as delivery vehicles to transport viruses to tumor sites, hiding the virus from the host immune system. Specifically, in the last decade, many studies have shown that cells with inherent tumor-tropic properties are very attractive candidates. Neural stem cells are being evaluated as carriers of oncolytic Ads for glioma therapy (Thaci et al. 2012), and CIK cells were employed to deliver the oncolytic vaccinia virus (Thorne et al. 2006). CIK cells, as infected carriers, have the potential to target cancer tissues and show no cytotoxicity against normal cells. They can bind tumor cells via the receptor natural killer group 2D (NKG2D) on the cell surface, resulting in a prolonged eclipse phase with the virus remaining hidden until interaction with the tumor (Thorne et al. 2006).

To optimize the use of anti-p21Ras scFv in the next phase of genetics-related cancer, we used CIK cells as an infected carrier of KGHV500 to mediate the anti-p21Ras scFv gene to treat the human lung cancer cell line xenograft in BALB/c mice by intravenous injection. We found that this combination therapy could obviously inhibit the growth of the xenograft tumors compared with the other groups in nude mice ($P < 0.01$). CIK cells as carriers can deliver KGHV500 into tumor cells effectively, and the anti-p21Ras scFv gene can be continuously and stably expressed together with the replication of KGHV500; in addition, no morphological changes occurred in normal organs and tissues.

Taken together, these results strongly suggest that CIK cells and KGHV500 may effectively and safely mediate the anti-p21Ras scFv gene for Ras-related lung cancer by an intravenous injection. Due to its low toxicity and good selectivity, this treatment can be extensively used for solid tumor metastasis that includes Ras alterations by an intravenous injection in the future. However, all the in vivo experiments were performed using the A549 cell line in BALB/c nude mouse, and the clinicopathologic and molecular features of these cells may be changed after a long period of culture in vitro. To be more representative of clinical trial results, establishing patient-derived xenograft models is our next goal, and then, we will be able to explore further possibilities of using combination therapy to carry the other exogenous anti-tumor genes or chemotherapeutic drugs. In conclusion, the possibility of using anti-p21Ras scFv to treat Ras-related cancer will also be an emphasis in our future research, and we firmly believe that anti-p21Ras scFv will provide the hope of improved health to cancer patients.

Funding The National Natural Science Foundation of China (no. 81460464), Applied Foundation Key Project of Yunnan Province (2018ZF008), and The Applied Basic Research Project Youth Foundation of Yunnan Province (no. 2017FD248).

Compliance with ethical standards

Conflict of interest The authors declare that they have no conflict of interest.

Ethical standards This study received the approval of the Ethics Board of 920th Hospital of the Joint Logistics Support Force of PLA and is also in accordance with the Helsinki Declaration of 1975. The animals involved in the study were cared for in accordance with institutional guidelines.

References

Andtbacka RH, Kaufman HL, Collichio F, Amatruda T, Senzer N, Chesney J, Delman KA, Spitler LE, Puzanov I, Agarwala SS (2015) Talimogene laherparepvec improves durable response rate in patients with advanced melanoma. J Clin Oncol 33(25):2780–2788

Casaluce F, Sgambato A, Sacco PC, Palazzolo G, Maione P, Rossi A, Ciardiello F, Gridelli C (2016) Resistance to crizotinib in advanced non-small cell lung cancer (NSCLC) with ALK rearrangement: mechanisms, treatment strategies and new targeted therapies. Curr Clin Pharmacol 11(2):77–87

Crino L, Weder W, van Meerbeeck J, Felip E, Group EGW (2010) Early stage and locally advanced (non-metastatic) non-small-cell lung cancer: ESMO Clinical Practice Guidelines for diagnosis, treatment and follow-up. Ann Oncol 21(Suppl 5):v103–115

Ferlay J, Soerjomataram I, Dikshit R, Eser S, Mathers C, Rebelo M, Parkin DM, Forman D, Bray F (2015) Cancer incidence and mortality worldwide: sources, methods and major patterns in GLOBOCAN 2012. Int J Cancer 136(5):E359–E386

Finke S, Trojaneck B, Lefterova P, Csipai M, Wagner E, Kircheis R, Neubauer A, Huhn D, Wittig B, Schmidt-Wolf IG (1998) Increase of proliferation rate and enhancement of antitumor cytotoxicity of expanded human CD3 + CD56 + immunologic effector cells by receptor-mediated transfection with the interleukin-7 gene. Gene therapy 5(1):31–39

Johnson L, Mercer K, Greenbaum D, Bronson RT, Crowley D, Tuveson DA, Jacks T (2001) Somatic activation of the K-ras

oncogene causes early onset lung cancer in mice. Nature 410(6832):1111–1116
Keedy V, Wang W, Schiller J, Chada S, Slovis B, Coffee K, Worrell J, Thet LA, Johnson DH, Carbone DP (2008) Phase I study of adenovirus p53 administered by bronchoalveolar lavage in patients with bronchioloalveolar cell lung carcinoma: ECOG 6597. J Clin Oncol 26(25):4166–4171
Kim CF, Jackson EL, Woolfenden AE, Lawrence S, Babar I, Vogel S, Crowley D, Bronson RT, Jacks T (2005) Identification of bronchioalveolar stem cells in normal lung and lung cancer. Cell 121(6):823–835
Kimura J, Ono HA, Kosaka T, Nagashima Y, Hirai S, Ohno S, Aoki K, Julia D, Yamamoto M, Kunisaki C et al (2013) Conditionally replicative adenoviral vectors for imaging the effect of chemotherapy on pancreatic cancer cells. Cancer Sci 104(8):1083–1090
Kohler J, Schuler M (2013) Afatinib, erlotinib and gefitinib in the first-line therapy of EGFR mutation-positive lung adenocarcinoma: a review. Onkologie 36(9):510–518
Köpinghöggård M, Tubulekas I, Guan H, Edwards K, Nilsson M, Vårum KM, Artursson P (2001) Chitosan as a nonviral gene delivery system. Structure–property relationships and characteristics compared with polyethylenimine in vitro and after lung administration in vivo. Gene Ther 8(14):1108–1121
Kotterman MA, Chalberg TW, Schaffer DV (2013) Viral vectors for gene therapy: translational and clinical outlook. Annu Rev Biomed Eng 17(1):63
Lara-Guerra H, Roth JA (2016) Gene therapy for lung cancer. Crit Rev Oncogol 21(1–2):115–124
Lowy DR, Willumsen BM (1993) Function and regulation of ras. Annu Rev Biochem 62(1):851
Lu C, Stewart DJ, Lee JJ, Ji L, Ramesh R, Jayachandran G, Nunez MI, Wistuba II, Erasmus JJ, Hicks ME (2012) Phase I clinical trial of systemically administered TUSC2(FUS1)-nanoparticles mediating functional gene transfer in humans. Plos One 7(4):e34833
Munn RJ, Marx PA, Yamamoto JK, Gardner MB (1985) Ultrastructural comparison of the retroviruses associated with human and simian acquired immunodeficiency syndromes. Lab Invest 53(2):194–199
Okudela K, Hayashi H, Ito T, Yazawa T, Suzuki T, Nakane Y, Sato H, Ishi H, Keqin X, Masuda A (2004) K-ras gene mutation enhances motility of immortalized airway cells and lung adenocarcinoma cells via Akt activation: possible contribution to non-invasive expansion of lung adenocarcinoma. Am J Pathol 164(1):91
Osborne CK, Neven P, Dirix LY, Mackey JR, Robert J, Underhill C, Schiff R, Gutierrez C, Migliaccio I, Anagnostou VK (2011) Gefitinib or placebo in combination with tamoxifen in patients with hormone receptor–positive metastatic breast cancer: a randomized phase II study. Clin Cancer Res 17(5):1147–1159
Ostapchuk P, Almond M, Hearing P (2011) Characterization of Empty adenovirus particles assembled in the absence of a functional adenovirus IVa2 protein. J Virol 85(11):5524–5531
Pan XY, Liu XJ, Li J, Zhen SJ, Liu DX, Feng Q, Zhao WX, Luo Y, Zhang YL, Li HW et al (2017) The antitumor efficacy of anti-p21Ras scFv mediated by the dual-promoter-regulated recombinant adenovirus KGHV300. Gene Ther 24(1):40–48
Parada LF, Tabin CJ, Shih C, Weinberg RA (1982) Human EJ bladder carcinoma oncogene is homologue of Harvey sarcoma virus ras gene. Nature 297(5866):474–478
Qin M, Escuadro B, Sharma S, Batra RK (2005) Gene transfer mediated by native versus fibroblast growth factor-retargeted adenoviral vectors into lung cancer cells. Am J Respir Cell Mol Biol 32(3):211–217
Shaw AT, Kim DW, Nakagawa K, Seto T, Crino L, Ahn MJ, De Pas T, Besse B, Solomon BJ, Blackhall F et al (2013) Crizotinib versus chemotherapy in advanced ALK-positive lung cancer. N Engl J Med 368(25):2385–2394
Siegel RL, Miller KD, Jemal A (2017) Cancer statistics. CA 67(1):7–30
Thaci B, Ahmed AU, Ulasov IV, Tobias AL, Han Y, Aboody KS, Lesniak MS (2012) Pharmacokinetic study of neural stem cell-based cell carrier for oncolytic virotherapy: Targeted delivery of the therapeutic payload in an orthotopic brain tumor model. Cancer Gene Ther 19(6):431
Thomas CE, Ehrhardt A, Kay MA (2003) Progress and problems with the use of viral vectors for gene therapy. Nat Rev Genet 4(5):346–358
Thorne SH, Negrin RS, Contag CH (2006) Synergistic antitumor effects of immune cell-viral biotherapy. Science 311(5768):1780
Urban JH, Merten CA (2011) Retroviral display in gene therapy, protein engineering, and vaccine development. ACS Chem Biol 6(1):61
Yan Y, Zhang YX, Fang WF, Kang SY, Zhan JH, Chen N, Hong SD, Liang WH, Tang YN, He DC (2015) Roles of immunohistochemical staining in diagnosing pulmonary squamous cell carcinoma. APJCP 16(2):551–557
Yang Z, Zhang Q, Xu K, Shan J, Shen J, Liu L, Xu Y, Xia F, Bie P, Zhang X et al (2012) Combined therapy with cytokine-induced killer cells and oncolytic adenovirus expressing IL-12 induce enhanced antitumor activity in liver tumor model. PloS One 7(9):e44802
Yang JL, Pan XY, Zhao WX, Hu QC, Ding F, Feng Q, Li GY, Luo Y (2016a) The antitumor efficacy of a novel adenovirus-mediated anti-p21Ras single chain fragment variable antibody on human cancers in vitro and in vivo. Int J Oncol 48(3):1218–1228
Yang JL, Liu DX, Zhen SJ, Zhou YG, Zhang DJ, Yang LY, Chen HB, Feng Q (2016b) A novel anti-p21Ras scFv antibody reacting specifically with human tumour cell lines and primary tumour tissues. BMC Cancer 16:131
Yu B, Zhang Y, Zhan Y, Zha X, Wu Y, Zhang X, Dong Q, Kong W, Yu X (2011) Co-expression of herpes simplex virus thymidine kinase and Escherichia coli nitroreductase by an hTERT-driven adenovirus vector in breast cancer cells results in additive antitumor effects. Oncol Rep 26(1):255–264

Publisher's Note Springer Nature remains neutral with regard to jurisdictional claims in published maps and institutional affiliations.